



Stability analysis of rock slopes using kinematic analysis and numerical modeling: Foça–Bağarası State Highway, Turkey

Mawuko Luke Yaw Ankah¹ · Cem Kincal²

Received: 20 April 2022 / Accepted: 17 June 2022 / Published online: 4 July 2022
© The Author(s), under exclusive licence to Springer Nature Switzerland AG 2022

Abstract

Slope failures along road cuts and highways pose significant threats to motorists and pedestrians. In this study, the stability of rock slopes along the Foça–Bağarası (FB) Highway in Turkey has been investigated using kinematic analysis and numerical modeling. The investigations were conducted at five survey stations along the highway. The results of the kinematic analysis showed that the joint sets at all the five stations along the FB Highway formed critical intersections that could result in wedge failures. Also, the kinematic analysis results showed significant toppling failure risks along the highway. The results of the finite element analysis showed that the slopes at some of the stations were in a critical state even without the influence of pore pressure. Also, the results showed that should the piezometric surface (or water table) rise to the mid-section of the slopes or higher, there would be a great likelihood of failures occurring. In addition, Strength Reduction Factor values calculated under seismic conditions showed that the slopes had a great vulnerability to seismic activity. The numerical modeling results were consistent with the kinematic analysis results as well as field observations and showed that the FB highway slopes stood a great risk of failure, especially during periods of major rainfall or seismic activity.

Keywords Rock slope stability · Highway · Kinematic analysis · Numerical modeling · Strength reduction factor

Introduction

Slope failures are geological hazards that could result in fatalities (Su et al. 2022; Tanoli et al. 2022). In this regard, over the years, significant efforts have been made by researchers across the globe to identify, predict, and ultimately mitigate slope stability problems (Yang et al. 2021; Gupta and Mukherjee 2022; Kundu et al. 2022). That notwithstanding, slope failures along road cuts and highways, for instance, continue to obstruct traffic and pose significant threats to motorists and pedestrians (Bushira et al. 2018; Zhao et al. 2018; Singh and Kumar 2020). Moreover, scores of people have sadly lost their lives as a result of unfortunate incidents of slope failures, especially due to the occurrences

of such failures in open-pit mines (Dash 2019; Mikroutsikos et al. 2021). This demonstrates the level of complexity involved in the quest to mitigate slope failures.

Many approaches have been developed and used for investigating rock slope failures. These include the empirical approach, which essentially consists of rock mass classification systems such as the Rock Quality Designation (RQD) (Deere 1963), the Rock Mass Rating (RMR) (Bieniawski 1989; Celada et al. 2014), the Q system (Barton et al. 1974; Barton and Bar 2015; Bar and Barton 2017), the Slope Mass Rating (SMR) (Romana 1985), and the Geological Strength Index (GSI) (Hoek 1994; Hoek et al. 1995; Marinos and Carter 2018).

The analytical approaches, such as the kinematic analysis, limit equilibrium analysis, and block theory approaches, are also commonly used to assess rock slope stability. Probabilistic methods are combined with the abovementioned analytical methods, should the need arise, to consider variations in discontinuity and intact rock properties and to estimate the probability of failure and reliability index for rock slopes. The kinematic analysis is typically performed using lower hemisphere or upper hemisphere stereonets. With the aid of such stereonets, kinematic analyses for various failure

✉ Mawuko Luke Yaw Ankah
mawuko.ankah1@gmail.com

¹ School of Resources and Environmental Engineering, Jiangxi University of Science and Technology, Ganzhou, Jiangxi 341000, People's Republic of China

² Geological Engineering Department, Engineering Faculty, Dokuz Eylül University, Tinaztepe Campus, 35160 Izmir, Turkey

modes can be effectively conducted. Kincal (2014), for example, successfully developed and made use of two new stereographic projection methods to perform slope stability analysis at an albite mine in Turkey. Likewise, Zheng et al. (2019a) developed a modified stereographic technique for kinematic (flexural toppling) analysis. Relatedly, Zheng et al. (2017) applied a probabilistic kinematic analysis procedure to an open-pit slope in the USA. Also, Alameda-Hernández et al. (2019) used close-range terrestrial digital photogrammetry and kinematic analysis to assess the stability of a rock slope in Spain. Recently, some other researchers have conducted studies on rock slope stability using the analytical approach. Zheng et al. (2019b), for example, used the limit equilibrium method (LEM) to investigate block-flexure toppling failure in rock slopes. Alemdag et al. (2021) used kinematic analysis and Geographic Information System (GIS)-based techniques to investigate rock fall potential along a motorway in Turkey. In the aforementioned study, Geographic Information System (GIS)-based instability maps were produced zoning the high-risk areas. Kundu et al. (2022) suggested a kinematic analysis procedure based on the Slope Mass Rating (SMR); the procedure (developed into a computer program called EasySMR) was applied to some rock slopes in India. Du et al. (2022) proposed a new analytical procedure for investigating rock slope stability; the suggested procedure was validated by applying it to rock slopes of the Dexing Copper Mine (China). In all the above-mentioned studies, various recommendations were suggested for ensuring the stability of the investigated slopes.

In addition to the empirical and analytical methods, numerical modeling (continuum and discontinuum) methods have successfully been used to solve complex rock slope stability problems. Continuum methods have been adopted by some researchers for investigations on rock slope stability. Jiang et al. (2015) used 3-D Strength Reduction Finite Element Method (FEM) to evaluate the stability of a complex rock slope in China while Pandit et al. (2018) used 2-D Finite Difference Method (FDM) to evaluate the stability of a gold mine pit slope in India. Similarly, Azarfar et al. (2019) used 3-D FDM to evaluate the stability of a mine pit slope and to model faults. Pradhan and Siddique (2020), as well, evaluated the stability of twenty rock slopes in the Himalayas using 2-D FEM; in their study, the slopes were categorized based on their stability state (strength reduction factor values) as either stable, quite stable, or unstable. Also, Liu et al. (2021) evaluated the stability of a limestone quarry slope in China using a finite difference code.

Some researchers have also used Discontinuum methods such as the Distinct Element Method (DEM) codes for investigating rock slope stability. Qi et al. (2016) evaluated the stability of a rock slope in China using 2-D DEM while Faramarzi et al. (2017) evaluated the stability of a power plant pit in Iran using 3-D DEM. Likewise, Dadashzadeh

et al. (2017) conducted a study on rock slope stability in Turkey using 3-D DEM and Response Surface (RS) method. Also, Li et al. (2018) used 3-D DEM and microseismic (MS) monitoring to assess the stability of a hydropower station (dam) slope in China while Wang et al. (2020) developed a procedure integrating statistics-based 3-D DEM and strength reduction methods for rock slope stability. Recently, Li et al. (2022) employed discrete fracture networks (DFN) in assessing the stability of a heavily fractured rock slope. Wu and Hsieh (2021) as well modeled the post-failure behavior of a landslide using the distinct element method.

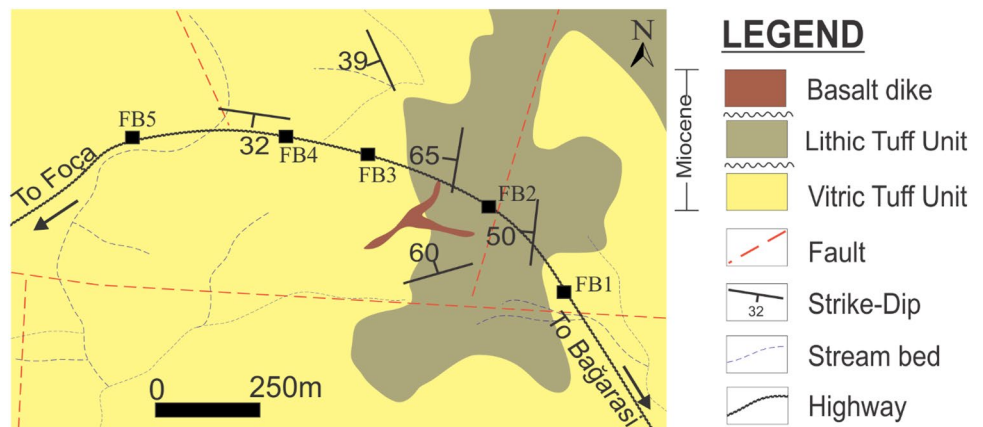
The foregoing discussion shows the various options that are available for assessing slope stability. It is important to note that the most appropriate method to use for slope stability analysis is usually determined by factors such as time and budgetary constraints as well as the degree of complexity of the problem. The empirical method, for instance, provides a quick and less expensive initial assessment of the stability of rock slopes since it is usually difficult to evaluate the stability of a rock slope in real time in both civil and mining engineering projects using the analytical or numerical modeling methods (Bar and Barton 2017). On the other hand, the analytical and numerical modeling approaches are best suited for comprehensive investigations of rock slope stability compared to the empirical approach.

In this study, the stability of rock slopes along the State highway between the towns of Foça and Bağarası (Turkey) has been investigated using kinematic analysis and numerical modeling. The main rock formation in the study area is volcanic tuffs which are known to be weak rocks and easily undergo weathering and deformation. Due to this, slope failures frequently occur along the highway; as a result of these failures, the road is usually blocked to traffic. In addition, these failures may cause significant harm to both life and property. This study, therefore, seeks to assess the stability of the rock slopes to help mitigate the slope failures along the State highway.

Description of the study area

The investigated rock slopes lie along the highway linking the towns of Foça and Bağarası in the northwestern part of Izmir (Turkey). Three different suites of volcanic rocks exist in the study area (Akay and Erdoğan 2004). These are (from youngest to oldest): The Foça alkaline volcanic rocks, Foca volcanic rocks, and the Yuntdag volcanic rocks. The lithological units mapped in the area as part of this study are andesitic lithic and vitric tuffs, rhyolitic lithic and vitric tuffs, basalt, rhyolite, and alluvion. The oldest lithological unit in the study area is the vitric tuff, which is overlain by the lithic tuff. Basalt dikes intrude the vitric and lithic tuffs. The rhyolite unit exists as domes within the volcanic tuffs. The lithological map of the study area is shown in Fig. 1.

Fig. 1 Lithological map of the study area with survey stations (FB1–FB5)



Materials and method

A detailed geotechnical (scanline) mapping was conducted on the rock slopes along the highway linking the towns of Foça and Bağarası, and discontinuity data were collected from the slope faces at a total of five stations (FB1–FB5) along the highway (see Fig. 1). Block samples of the rock units were also collected from the field. The block samples were then drilled in the laboratory to obtain core samples with a length to diameter ratio of 2:1. These prepared core samples were then tested in the laboratory to obtain the physico-mechanical properties of the rock materials such as unit weight and compressive strength. Kinematic analysis was conducted using Dips 7.0 software (Rocscience 2019) to identify the potential plane, wedge, and toppling failures along the highway. The two essential parameters used for conducting the kinematic analyses are the discontinuity orientation data (obtained from the scanline mapping) and the discontinuity friction angle. The mean discontinuity friction angle of the rock units (volcanic tuffs) along the Foça–Bağarası (FB) Highway was determined from direct shear tests to be 30°. The stability of the rock slopes was also assessed using numerical modeling (finite element analysis). The behavior of the slopes was modeled under various conditions of saturation and seismic activity using Rs²(Phase²) software (Rocscience 2014). The intact rock and rock mass were modeled using the Generalized Hoek–brown criterion and the rock material was treated as elastoplastic. The rock mass properties were estimated based on field conditions and laboratory results using Rocdata software (Rocscience 2016). In the numerical modeling, the shear strength reduction (SSR) method was used to calculate strength Reduction Factors (SRF) (akin to Factor of Safety values) for the various slopes under gravity stresses as well as saturated and dry conditions. In this way, detailed information was obtained about the behavior of the various slopes in response to pore pressure and seismic activity. It is important to note

that the study area is an earthquake-prone region. For this reason, the numerical modeling was also conducted under seismic (positive to right direction of seismic waves) conditions using peak ground acceleration (PGA) values of 0.1 g and 0.2 g. Figure 2a shows one of the slopes (FB1) which was modeled. The original model of slope FB1 is shown in Fig. 2b.

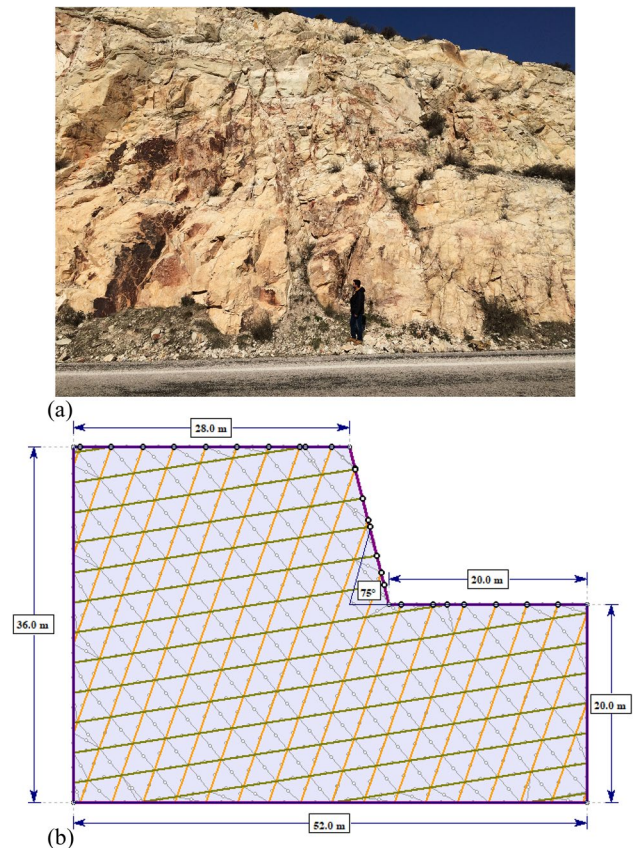


Fig. 2 Slope at station FB1: **a** actual slope; **b** original model

Results and discussion

Kinematic analysis

The polar equal area (lower hemisphere) plots of the discontinuities mapped at the five stations (FB1-FB5) along the highway are shown in Fig. 3. The orientations of the dominant joint sets in Fig. 3 as well as the respective slope orientation data used to conduct the kinematic analysis are presented in Table 1. The results of the kinematic analysis conducted for the various stations along the FB Highway (see Table 2) show significant risks of the plane, wedge,

and toppling failures along the FB Highway. The percentages of critical discontinuities that can result in plane failures range from 15.66%(FB1) to as high as 50.00%(FB3). The severity of the plane failure risks can be better appreciated by considering the contributions of the mean joint sets (J1-J4) to potential plane failures. Results of such an analysis indicate that all poles (100%) of Joint sets 2 (J2) at stations FB1 and FB4 are at risk of plane failure. Similarly, all joint poles of joint sets J1(FB3) and J3(FB5) as well as 81.25% of poles in joint set J4(FB2) fall within the plane sliding zone.

Also, Table 2 results show that the joint sets at all the five stations along the FB Highway form critical intersections

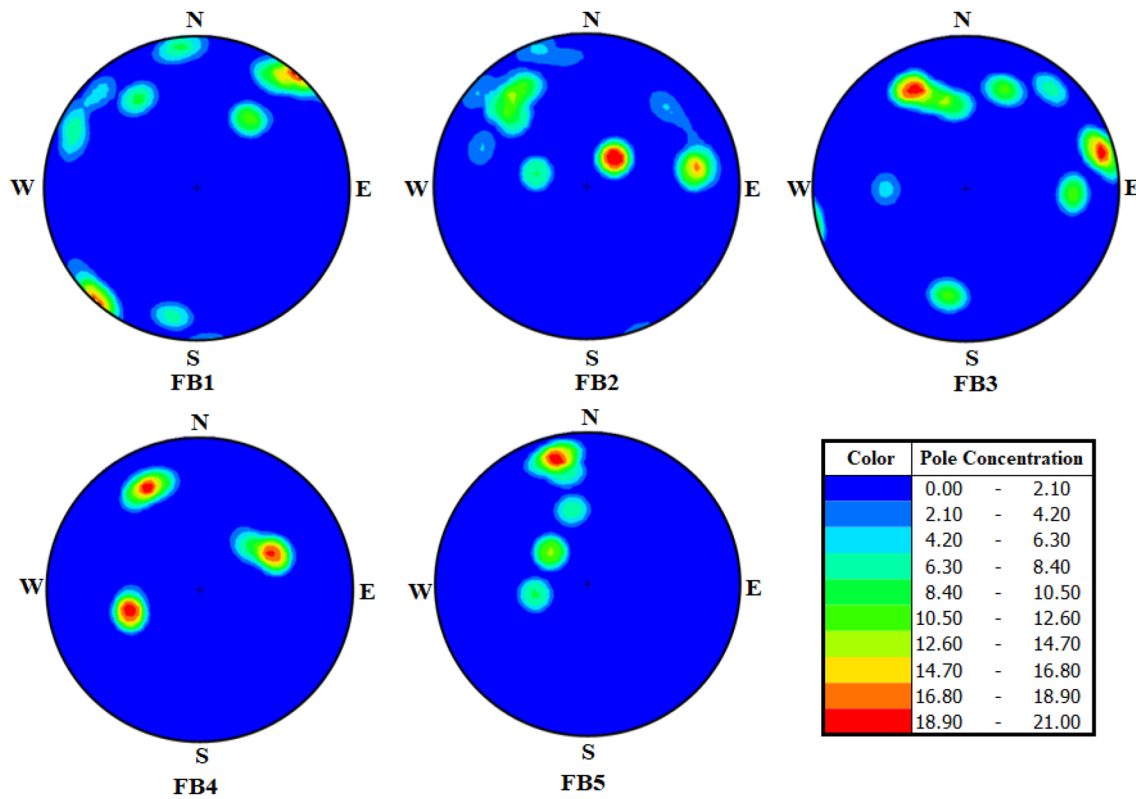


Fig. 3 The polar equal area plots of the discontinuities mapped at the five stations

Table 1 Orientation data of slopes and joint sets

Slope ID	Mean orientation of dominant Joint sets (J_i) (Dip direction/dip angle)- Degrees				Slope orientation (Dip direction/dip angle)-degrees	Total number of joint poles
	J_1	J_2	J_3	J_4		
FB1	221/87	218/48	359/89	142/66	217/75	166
FB2	259/63	225/21	104/28	138/65	138/74	98
FB3	158/56	209/64	260/74	9/60	152/74	96
FB4	240/42	153/64	73/40	–	153/72	90
FB5	79/29	131/26	168/41	167/73	145/75	81

Table 2 The kinematic analysis results for the FB highway slopes

Slope ID	Plane sliding			Wedge sliding			Toppling		
	Cri	T	%	*Cri	*T	%	Cri	T	%
FB1	26	166	15.66	3	6	50	40	166	24.1
FB2	30	98	30.61	3	6	50	0	98	0
FB3	48	96	50.00	4	6	66.67	0	96	0
FB4	38	90	42.22	2	3	66.67	0	90	0
FB5	32	81	39.5	2	6	33.33	0	81	0

Contributions of dominant joint sets to potential failures			
FB1	J1(2/64), J2(22/22), J4(2/24)	I ₁₂ , I ₂₃ , I ₂₄	J1(28/64), J2(12/32)
FB2	J4(26/32)	I ₂₄ , I ₁₄ , I ₃₄	–
FB3	J1(34/34), J2(10/16),	I ₁₂ , I ₁₃ , I ₁₄ , I ₂₃	–
FB4	J1(4/34), J2(30/30), J3(4/26)	I ₁₂ , I ₂₃	–
FB5	J1(6/12), J3(10/10), J4(16/41)	I ₁₄ , I ₂₄	–

Cri. Critical number of discontinuities, **Cri*. Critical number of mean set plane intersections, *T* Total number of discontinuities, **T* Total number of mean set plane intersections

Ji(a/b) ‘a’ joint poles out of a total of ‘b’ in joint set Ji contributing to potential failures, *I_{ij}* wedge sliding on joints *i* and *j* along *I_{ij}*

that can result in wedge failures. The percentages of critical mean joint intersections that can cause wedge sliding range from 33.33%, for station FB5, to 66.67% for stations FB3 and FB4. Stations FB1 and FB2 have half of the mean joint intersections contributing to wedge failures while that of station FB5 is one-third.

In regard to toppling failure potential along the FB Highway, station FB1 shows significant toppling failure risks while the rest of the stations (FB2–FB5) virtually have no such risks with respect to toppling. A potential toppling failure observed at station FB1 is shown in Fig. 4a; this field observation is consistent with the toppling failure analysis for station FB1 (see Fig. 4b), which shows a significant concentration of poles in the toppling failure region.

Finite element analysis

The numerical models of the FB Highway slopes (incorporating the most critical joints) are shown in Fig. 5. The physico-mechanical properties of the rock materials from the various stations as well as the strength reduction factor (SRF) values obtained from the numerical modeling are presented in Table 3. The numerical modeling results (see Table 3) show that under dry conditions, the computed SRF values ranged from 0.9(station FB2) to 1.43(station FB5). Also, the results show that the slopes at stations FB1, FB2, and FB4 (SRF values less than 1.2) are in a critical state even without the influence of pore pressure. On the other hand, the results show that station FB3 (SRF value of 1.3),

Fig. 4 Toppling failure investigation at Station FB1: **a** Observed potential toppling failure; **b** Toppling failure analysis

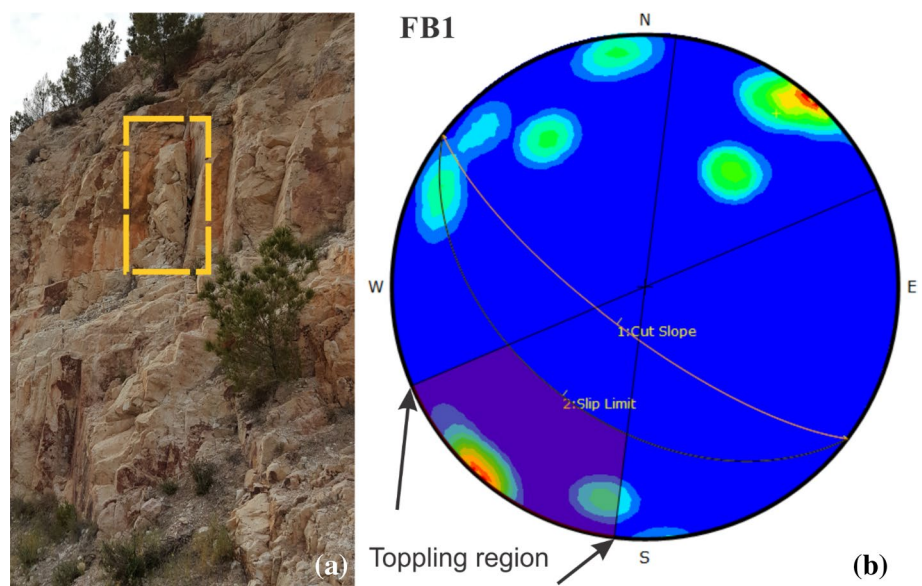
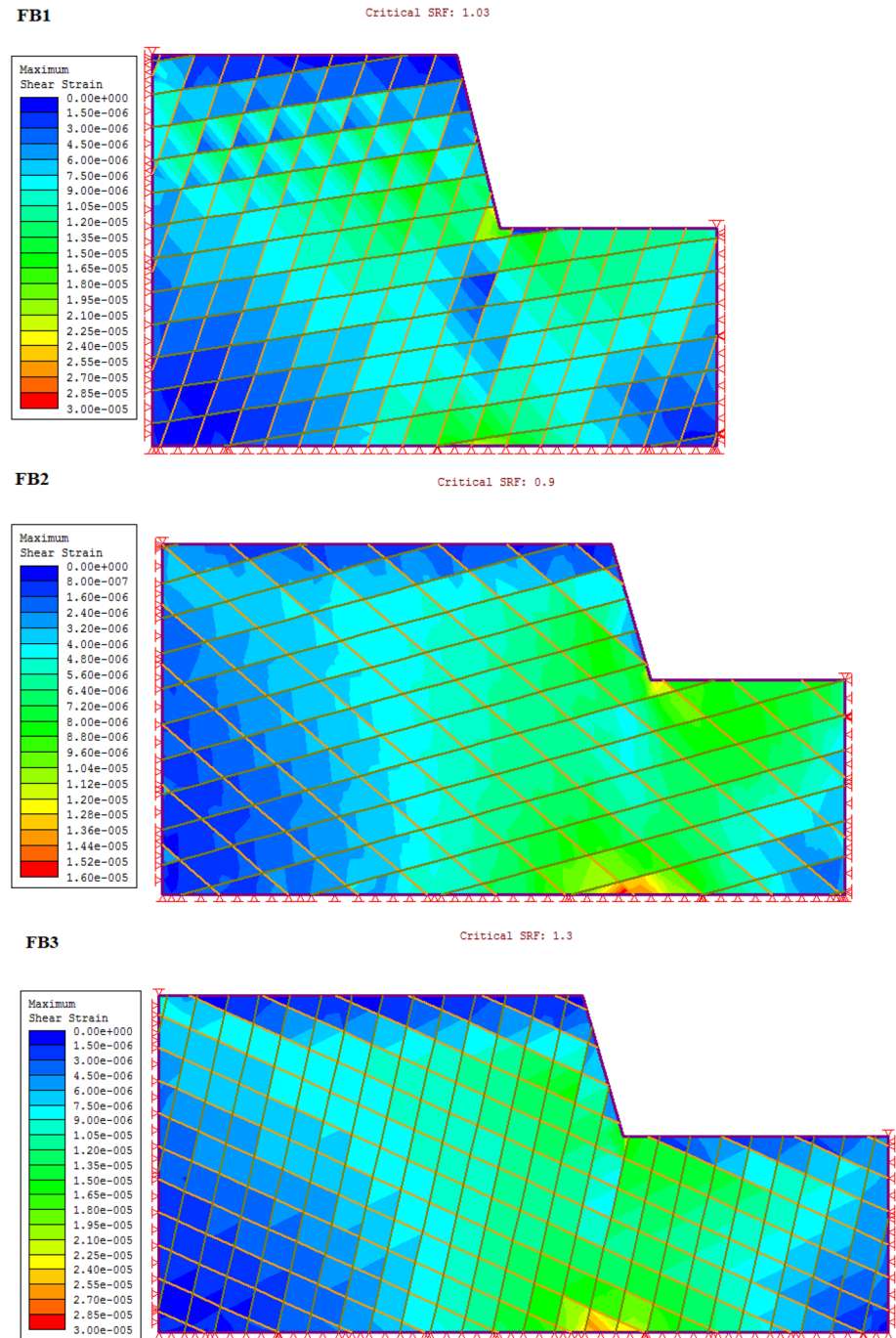


Fig. 5 The numerical models of the FB Highway slopes (stations FB1–FB5)



as well as station FB5 (SRF value of 1.43), is likely to be stable when the slope is in a dry state. Notably, reductions in SRF occurred in all the slopes when computations for SRF were done with the piezometric surface (or water table) at the mid-section of the slope (see Table 3). Under this condition, SRF values for station FB1 reduced from 1.03 to 0.88 while that of station FB2 decreased from 0.9 to 0.84. Also, under the same condition, SRF values reduced from 1.3 to 1.2 and from 0.93 to 0.84 for stations FB3 and FB4, respectively, while that of station FB5 decreased from 1.43

to 1.28. Clearly, should the piezometric surface (or water table) rise to the mid-section of the slopes, there will be a great likelihood of failures occurring.

Similarly, significant reductions in SRF were recorded in all the slopes (FB1–FB5) when SRF was calculated with the piezometric surface at the top of the slope; all the slopes had SRF values less than 1 and will most likely fail under this condition. In addition, SRF values which were calculated under seismic conditions (assuming the slopes are in a dry state) show a great effect of seismic activity on the slopes.

Fig. 5 (continued)

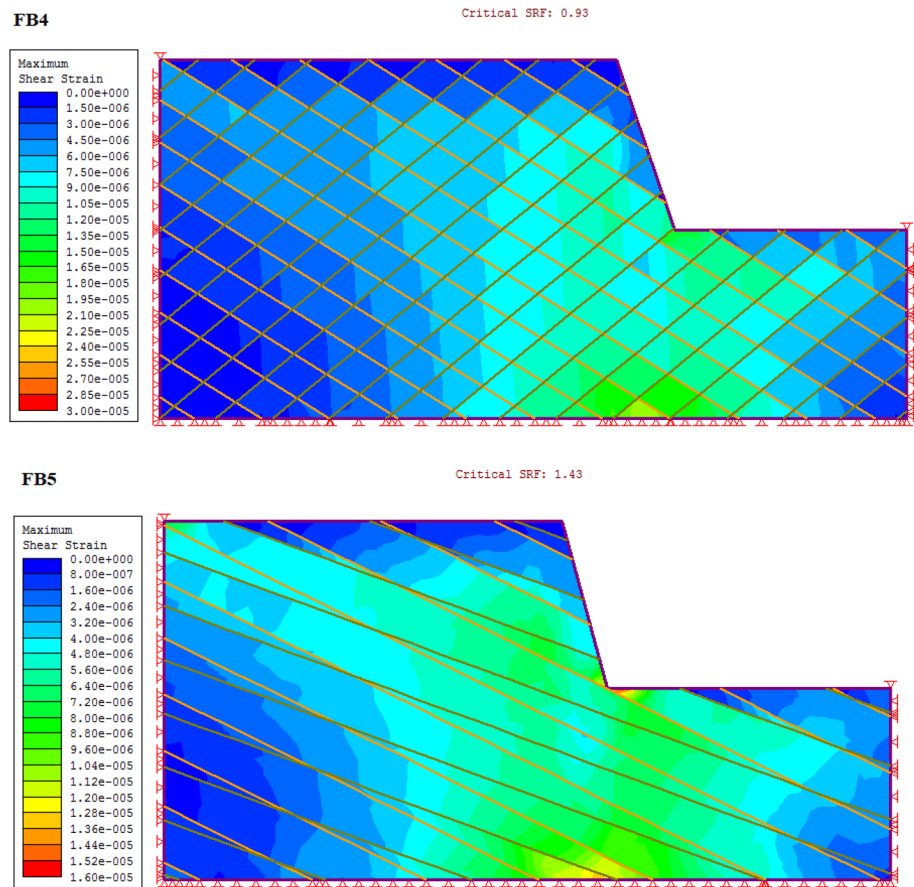


Table 3 SRF values of the slopes under various conditions

Slope ID/Property	FB1	FB2	FB3	FB4	FB5
Unit weight (g/cm ³)	1.76	2.05	1.78	1.87	2.09
Uniaxial compressive strength (MPa)	25.32	40.66	13.25	16.89	26.95
SRF values					
Gravitational loading					
Dry/Piezometric line at toe of slope	1.03	0.9	1.3	0.93	1.43
Piezometric line at middle of slope	0.88	0.84	1.2	0.84	1.28
Piezometric line at top of slope	0.79	0.75	0.93	0.7	0.93
Seismic loading					
0.1 g	0.91	0.74	1.01	0.76	1.14
0.2 g	0.76	0.61	0.82	0.62	0.93

With a peak ground acceleration (PGA) of 0.1 g, SRF values ranged between 0.74(FB2) and 1.14 (FB5) while with a PGA of 0.2 g calculated SRF values for FB1–FB5 were all less than 1. The obtained results show that the slopes have a great vulnerability to seismic activity. Thus, the numerical modeling results are consistent with that obtained from the

kinematic analysis and show that the FB highway slopes stand a great risk of failure, especially during periods of major rainfall or seismic activity.

Conclusion

In this study, the stability of rock slopes along the State highway between the towns of Foça and Bağarası (Turkey) was assessed using kinematic analysis and numerical modeling. The investigations were conducted at five stations (FB1–FB5) along the FB highway.

The kinematic analysis results showed significant risks of the plane, wedge, and toppling failures along the FB Highway. The percentages of critical discontinuities that could cause plane failures ranged from 15.66%(FB1) to as high as 50.00%(FB3). Similarly, the obtained results indicated that the joint sets at all the five stations along the FB Highway formed critical intersections that could result in wedge failures. Also, the kinematic analysis results showed significant toppling failure risks at Station FB1. However, the results indicated that the chances of toppling failures occurring at stations FB2–FB5 were low.

The numerical modeling results showed that the slopes at stations FB1, FB2, and FB4 (SRF values less than 1.2) were in a critical state even without the influence of pore pressure. However, the results showed that stations FB3 (SRF value of 1.3) and FB5 (SRF value of 1.43) were likely to be stable should the slope be in a dry state. Significant reductions in SRF were observed in all the slopes when calculations for SRF were done with the piezometric surface (or water table) at the mid-section of the slope and at the top section of the various slopes. This implies that should the piezometric surface (or water table) rise to the mid-section of the slopes or higher, there would be a great likelihood of failures occurring. Also, SRF values calculated under seismic conditions showed that the slopes had a great vulnerability to seismic activity. The numerical modeling results were consistent with the kinematic analysis results as well as field observations and showed that the FB highway slopes stood a great risk of failure, especially during periods of major rainfall or seismic activity.

Based on the results obtained, it is necessary to regularly monitor the FB Highway slopes and remove loose rock materials from the slope face. Ditches are also required to hold on to falling rocks, especially at station FB1. In addition, the construction of retaining walls should be considered to protect the traffic from the danger caused by falling blocks.

Data availability The datasets produced during and/or analyzed during this study are available from the corresponding author upon reasonable request.

Declarations

Conflict of interest The authors would like to state that they have no conflict of interest to declare.

References

- Akay E, Erdoğ an B (2004) Evolution of Neogene calc-alkaline to alkaline volcanism in the Aliağa-Foça region (Western Anatolia, Turkey). *J Asian Earth Sci* 24(3):367–387
- Alameda-Hernández P, El Hamdouni R, Irigaray C, Chacón J (2019) Weak foliated rock slope stability analysis with ultra-close-range terrestrial digital photogrammetry. *Bull Eng Geol Env* 78(2):1157–1171. <https://doi.org/10.1007/s10064-017-1119-z>
- Alemdag S, Bostanci HT, Gacener E (2021) GIS-based determination of potential instabilities and source rock areas on the Torul-Kürtün (Gümüşhane) motorway, rockfall, and protection structure analyses. *Bull Eng Geol Env* 81(1):30. <https://doi.org/10.1007/s10064-021-02498-7>
- Azarfar B, Ahmadvand S, Sattarvand J, Abbasi B (2019) Stability analysis of rock structure in large slopes and open-pit mine: numerical and experimental fault modeling. *Rock Mech Rock Eng* 52(12):4889–4905
- Bar N, Barton N (2017) The Q-slope method for rock slope engineering. *Rock Mech Rock Eng* 50(12):3307–3322
- Barton N, Bar N (2015) Introducing the Q-slope method and its intended use within civil and mining engineering projects. In *ISRM Regional Symposium-EUROCK 2015*
- Barton N, Lien R, Lunde J (1974) Engineering classification of rock masses for the design of tunnel support. *Rock Mech* 6(4):189–236
- Bieniawski ZT (1989) Engineering rock mass classifications: a complete manual for engineers and geologists in mining, civil, and petroleum engineering. John Wiley & Sons
- Bushira KM, Gebregiorgis YB, Verma RK, Sheng Z (2018) Cut soil slope stability analysis along national Highway at wozeka-gidole road, Ethiopia. *Model Earth Syst Environ* 4(2):591–600
- Celada B, Tardáguila I, Varona P, Rodríguez A, Bieniawski Z (2014) Innovating tunnel design by an improved experience-based RMR system. In: *Proceedings of the world tunnel congress*, pp 1–9
- Dadashzadeh N, Duzgun HSB, Yesiloglu-Gultekin N (2017) Reliability-based stability analysis of rock slopes using numerical analysis and response surface method. *Rock Mech Rock Eng* 50(8):2119–2133
- Dash AK (2019) Analysis of accidents due to slope failure in Indian opencast coal mines. *Curr Sci* 117(2):304
- Deere D (1963) Technical description of rock cores for engineering purpose. *Rock Mech Eng Geol* 1(1):17–22
- Du SG, Saroglou C, Chen Y, Lin H, Yong R (2022) A new approach for evaluation of slope stability in large open-pit mines: a case study at the Dexing Copper Mine, China. *Environ Earth Sci* 81(3):102. <https://doi.org/10.1007/s12665-022-10223-0>
- Faramarzi L, Zare M, Azhari A, Tabaei M (2017) Assessment of rock slope stability at Cham-Shir Dam Power Plant pit using the limit equilibrium method and numerical modeling. *Bull Eng Geol Env* 76(2):783–794
- Gupta AK, Mukherjee MK (2022) Evaluating road-cut slope stability using newly proposed stability charts and rock microstructure: an example from Dharasu-Uttarkashi Roadway Lesser Himalayas India. *Rock Mech Rock Eng*. <https://doi.org/10.1007/s00603-022-02846-3>
- Hoek E (1994) Strength of rock and rock masses. *ISRM News J* 2.4–16
- Hoek E, Kaiser P, Bawden W (1995) Support of underground excavation in hard rock: Rotterdam. AA Balkema, Rotterdam
- Jiang Q, Qi Z, Wei W, Zhou C (2015) Stability assessment of a high rock slope by strength reduction finite element method. *Bull Eng Geol Env* 74(4):1153–1162
- Kıncal C (2014) Application of two new stereographic projection techniques to slope stability problems. *Int J Rock Mech Min Sci* 66:136–150
- Kundu J, Sarkar K, Verma A, Singh TN (2022) Novel methods for quantitative analysis of kinematic stability and slope mass rating in jointed rock slopes with the aid of a new computer application. *Bull Eng Geol Env* 81(1):1–19
- Li B, Li T, Xu N, Dai F, Chen W, Tan Y (2018) Stability assessment of the left bank slope of the Baihetan Hydropower Station, Southwest China. *Int J Rock Mech Min Sci* 104:34–44
- Li X, Liu J, Gong W, Xu Y, Bowa VM (2022) A discrete fracture network based modeling scheme for analyzing the stability of highly fractured rock slope. *Comput Geotech* 141:104558
- Liu K, Li H, Pang S, Mi M, Chen J, Sun K (2021) Numerical simulation analysis of slope instability and failure of limestone mine in Weibei. *Adv Civil Eng* 2021:1–14
- Marinos V, Carter TG (2018) Maintaining geological reality in application of GSI for design of engineering structures in rock. *Eng Geol* 239:282–297
- Mikroutsikos A, Theocharis A, Koukouzas N, Zevgolis I (2021) Slope stability of deep surface coal mines in the presence of a weak zone. *Geomech Geophys Geo-Energy Geo-Resour* 7(3):1–17

- Pandit B, Tiwari G, Latha GM, Sivakumar Babu GL (2018) Stability analysis of a large gold mine open-pit slope using advanced probabilistic method. *Rock Mech Rock Eng* 51(7):2153–2174
- Pradhan SP, Siddique T (2020) Stability assessment of landslide-prone road cut rock slopes in Himalayan terrain: a finite element method based approach. *J Rock Mech Geotech Eng* 12(1):59–73
- Qi C, Wu J, Liu J, Kanungo DP (2016) Assessment of complex rock slope stability at Xiari, southwestern China. *Bull Eng Geol Env* 75(2):537–550
- Rocscience (2014) Phase2 version 8.020, finite element analysis for excavations and slopes. In: Rocscience Inc. Ontario
- Rocscience (2016) RocData v5.002 - Rock, Soil and Discontinuity Strength Analysis. Ontario, Canada
- Rocscience (2019) Dips v7.0 graphical and statistical analysis of orientation data. Toronto, Ontario, Canada
- Romana M (1985) New adjustment ratings for application of Bieniawski classification to slopes. In *Proceedings of the international symposium on role of rock mechanics, Zacatecas, Mexico*, pp 49–53
- Singh K, Kumar V (2020) Road-cut Slope stability assessment along Himalayan National Highway NH-154A, India. *J Geol Soc India* 96(5):491–498
- Su Z, Wang G, Wang Y, Luo X, Zhang H (2022) Numerical simulation of dynamic catastrophe of slope instability in three Gorges reservoir area based on FEM and SPH method. *Nat Hazards* 111(1):709–724. <https://doi.org/10.1007/s11069-021-05075-z>
- Tanoli JI, Chen N, Ullah I, Qasim M, Ali S, Rehman Qu, Umber U, Jadoon IAK (2022) Modified “Rockfall Hazard Rating System for Pakistan (RHRSP)”: an application for hazard and risk assessment along the Karakoram Highway, Northwest Pakistan. *Appl Sci* 12(8):3778
- Wang H, Zhang B, Mei G, Xu N (2020) A statistics-based discrete element modeling method coupled with the strength reduction method for the stability analysis of jointed rock slopes. *Eng Geol* 264:105247
- Wu J-H, Hsieh P-H (2021) Simulating the postfailure behavior of the seismically-triggered Chiu-fen-erh-shan landslide using 3DEC. *Eng Geol* 287:106113
- Yang Y, Xia Y, Zheng H, Liu Z (2021) Investigation of rock slope stability using a 3D nonlinear strength-reduction numerical manifold method. *Eng Geol* 292:106285
- Zhao H, Tian WP, Li JC, Ma BC (2018) Hazard zoning of trunk highway slope disasters: a case study in northern Shaanxi, China. *Bull Eng Geol Env* 77(4):1355–1364
- Zheng J, Kulatilake PHSW, Shu B (2017) Improved probabilistic kinematic analysis procedure based on finite size discontinuities and its application to a rock slope at open pit mine in US. *Int J Geomech* 17(2):04016052
- Zheng J, Lü Q, Deng J, Yang X, Fan X, Ding Z (2019a) A modified stereographic projection approach and a free software tool for kinematic analysis of rock slope toppling failures. *Bull Eng Geol Env* 78(7):4757–4769
- Zheng Y, Chen C, Liu T, Zhang H, Sun C (2019b) Theoretical and numerical study on the block-flexure toppling failure of rock slopes. *Eng Geol* 263:105309

Publisher's Note Springer Nature remains neutral with regard to jurisdictional claims in published maps and institutional affiliations.